The Canadian Mineralogist
Vol. 43, pp. 387-407 (2005)

SYNDEFORMATIONAL EMPLACEMENT OF A TONALITIC SHEET-COMPLEX IN A LATE-VARISCAN THRUST REGIME: FABRICS AND MECHANISM OF INTRUSION, MONTE'E SENES, NORTHEASTERN SARDINIA, ITALY

JÖRN H. KRUHL[§]

Tectonics and Material Fabrics Section, Faculty of Civil and Geodetic Engineering, Technische Universität München, D–80290 München, Germany

RON H. VERNON

Department of Earth and Planetary Sciences and National Key Centre for GEMOC, Macquarie University, Sydney, NSW 2109, Australia

ABSTRACT

The Monte'e Senes intrusive complex in northeastern Sardinia represents a good example of a syntectonic tonalitic sheet-complex. Its history consists of at least three intrusive events involving tonalitic magma and one subsequent intrusive event involving leucogranitic magma. The tonalites form numerous cm- to m-thick layers subparallel to the main foliation and layering of the country rocks. Emplacement occurred under greenschist-facies conditions of the country rocks. Deformation fabrics and fabrics of the contact aureole provide information on kinematics and P–T conditions during intrusion, as well as the relationship to the regional deformation. High-T deformation fabrics of quartz and plagioclase in the intrusive bodies, together with magmatic and high-T foliations and lineations parallel to foliations and lineations of the country rocks, indicate syntectonic intrusion. The deformation of cordierite, andalusite and sillimanite in the contact aureole, as well as the high-T deformation of quartz, point to a long-lasting history of partly synchronous deformation and intrusion. A relatively shallow intrusive body is indicated by the occurrence of andalusite and cordierite in the contact aureole and by granophyric microstructures. Greenschist-facies deformation fabrics in all of the igneous rocks indicate that the intrusion was outlasted by the regional deformation. The Monte'e Senes complex was emplaced during retrograde metamorphism associated with west-directed thrusting of the late Variscan continent–continent collision between Gondwana and Armorica.

Keywords: andalusite, cation leaching, contact metamorphism, cordierite, corundum, deformation, foliation, granite, microfabrics, sheets, sillimanite, syntectonic intrusion, tonalite, Sardinia, Italy.

SOMMAIRE

Le complexe intrusif de Monte'e Senes, dans le nord-est de la Sardaigne, en Italie, représenterait un bel exemple d'un complexe tonalitique syntectonique mis en place en feuillets. Nous distinguons au moins trois événements intrusifs impliquant un magma tonalitique, et une venue tardive de magma leucogranitique. Les tonalites se présentent en de nombreux feuillets centimétriques à métriques subparallèles à la foliation principale et au litage de l'encaissant. La mise en place s'est déroulée aux conditions du faciès schistes verts dans l'encaissant. Les microstructures dues à la déformation, ainsi que celles développées dans l'auréole de contact, fournissent des indices de la cinématique et des conditions P–T au cours de l'intrusion, et de la relation avec la déformation à l'échelle régionale. Les microstructures dues à la déformation du quartz et du plagioclase à température élevée, ainsi que les foliations et linéations magmatiques et de haute température parallèles à celles dans l'encaissant, sont des indications d'une intrusion syntectonique. La déformation de la cordiérite, de l'andalusite et de la sillimanite dans l'auréole de contact, de même que la déformation du quartz à température élevée, indiquent une période de déformation étalée dans le temps, en partie synchrone avec la déformation régionale et l'activité intrusive. Une mise en place à relativement faible profondeur serait responsable de la présence de l'andalousite et de la cordiérite dans l'auréole de contact, et de microstructures granophyriques dans les roches intrusives. Les microstructures dues à la déformation au faciès schistes verts partout dans les roches intrusives montrent que la déformation régionale a continué après la mise en place. Le complexe de Monte'e Senes fut mis en place lors d'un épisode de métamorphisme rétrograde associé à un chevauchement vers l'ouest lors d'une collision de Gondwana et Armorique à l'époque varisque tardive.

(Traduit par la Rédaction)

Mots-clés: andalousite, lessivage de cations, métamorphisme de contact, cordiérite, corindon, déformation, foliation, granite, microstructures, intrusion en feuillets, sillimanite, intrusion syntectonique, tonalite, Sardaigne, Italie.

[§] *E-mail address*: kruhl@tum.de

Introduction

In this paper, we present evidence of (1) intrusion of a felsic magma and contact metamorphism to the hornblende-hornfels facies occurring during regional deformation, (2) intrusion of sheets parallel to the foliation in the country rocks, and (3) hydrogen metasomatism during contact metamorphism. We describe relationships among the intrusive bodies, contact metamorphism and regional deformation at Monte'e Senes, Sardinia, where a biotite tonalite and several minor granitic bodies have intruded pelitic and psammitic schists that had previously been regionally metamorphosed to greenschist-facies conditions. Our study is based on a combination of structural investigation on the outcrop scale, thin-section observations of reaction textures and deformation microstructures, and of measurements of crystallographic preferred orientation.

Geological Framework

The Monte'e Senes region is part of the northernmost Nappe Zone (Carmignani *et al.* 1994) of the Sardinian Variscides (Fig. 1). This zone is interpreted as being built of Ordovician sedimentary units (Beccaluva *et al.* 1985) along an early Paleozoic active continental margin (Memmi *et al.* 1983). The sedimentary rocks underwent Variscan deformation and low- to

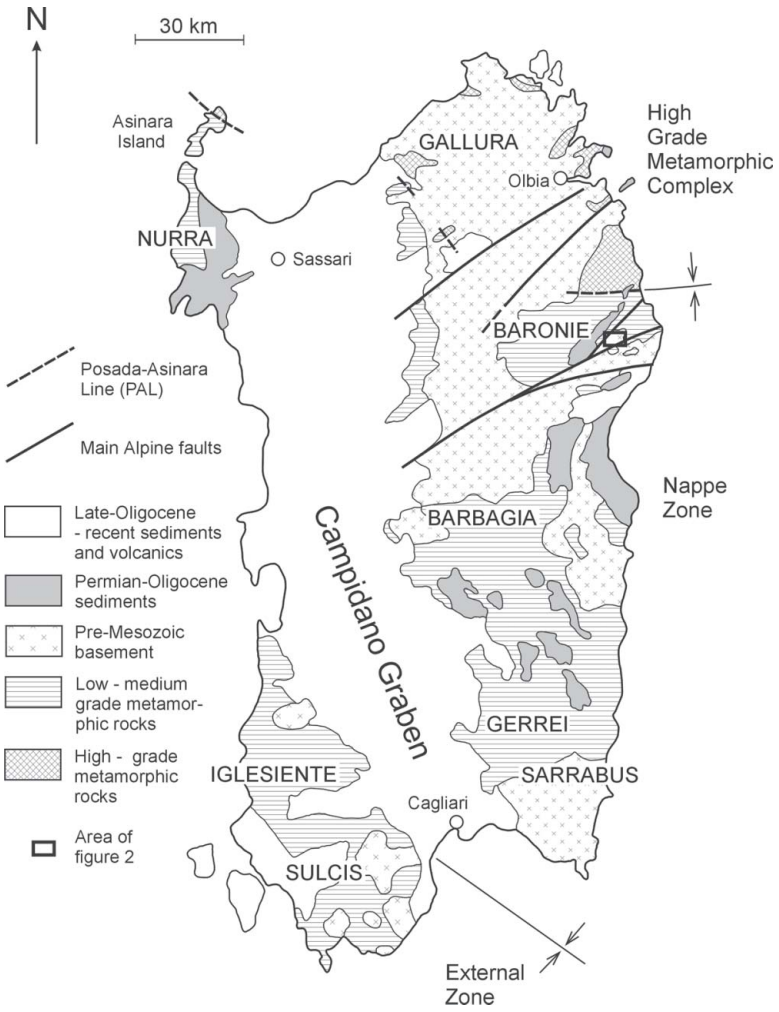

FIG. 1. Large-scale geological structure of Sardinia, modified after Cappelli *et al.* (1991) and Carmignani *et al*. (1992).

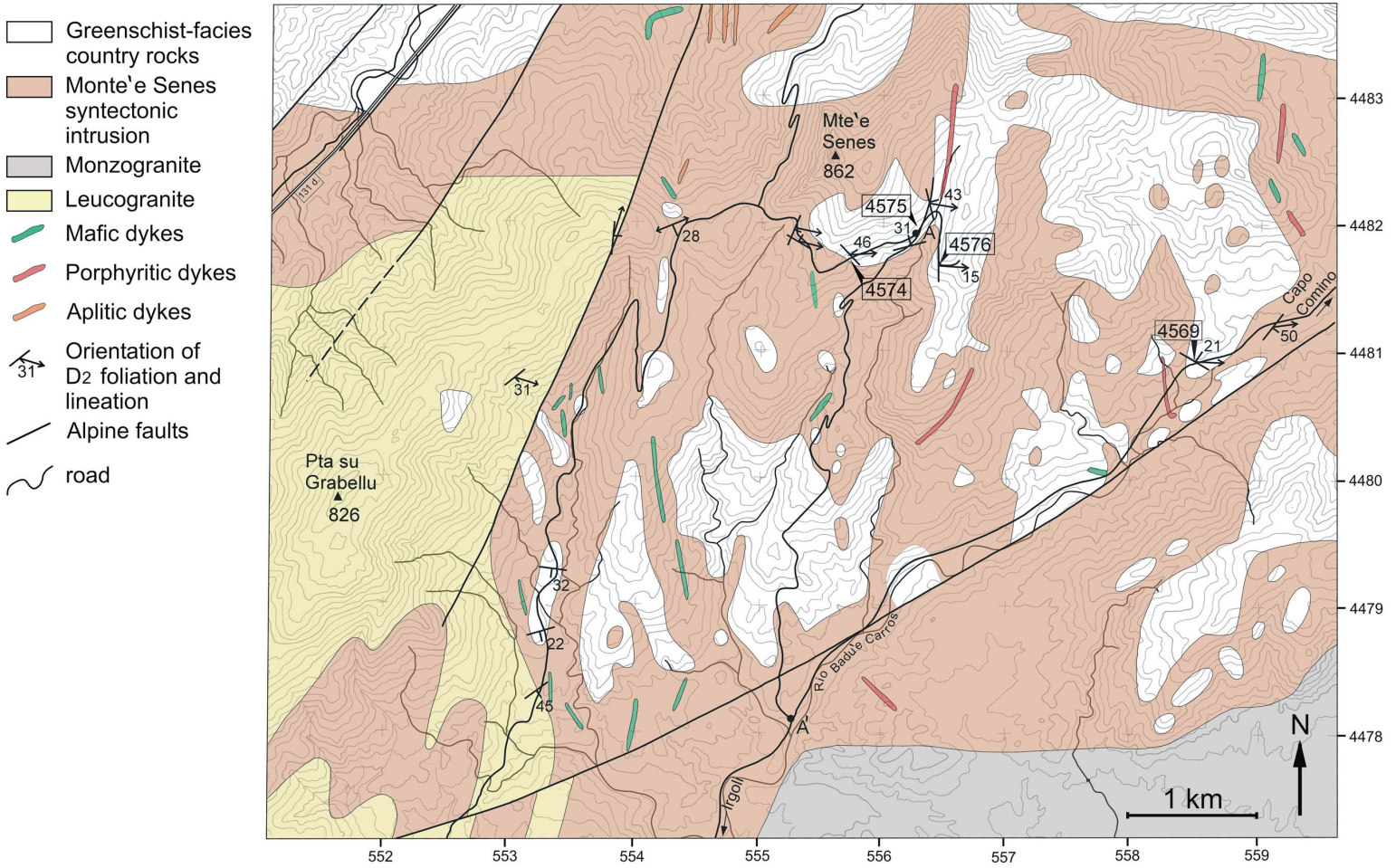

FIG. 2. Geology of the Monte'e Senes region, modified after Carta Geologica della Sardegna, 1:200000, Foglio Nord, Servizio Geologico Nazionale, and Carta Geologica d'Italia, 1:100000, Foglio 195. Numbers of outcrops mentioned in the text and representative orientations of foliation and lineation in the syndeformational granitic rocks and wallrocks are indicated. The rock column, sketched in Figure 4, has been constructed on the basis of measurements along the road A–A'. Interval of contour lines = 25 m.

medium-grade metamorphism. They were locally syntectonically intruded by igneous rocks of various compositions. Subsequently, most of the Sardinian Variscan metamorphic rocks were intruded by granitic rocks of the Sardic–Corsic Batholith *ca.* 300–280 Ma ago (Del Moro *et al.* 1975). The metamorphic and igneous rocks were uplifted, partly exhumed, and then covered by post-Carboniferous sedimentary units. The Alpine orogeny led to large-scale faulting and brittle strike-slip shear zones, but not to metamorphism. The main geological relationships among igneous rocks, country rocks and Alpine faulting in the Monte'e Senes region are shown in Figure 2.

Tectonics and Metamorphism of the Country Rocks away from the Intrusive Body

Rocks outside the contact metamorphic aureole of the Monte'e Senes complex are fine-grained schists, mylonites, quartzites and marbles, including muscovite – chlorite – quartz – plagioclase – graphite schist, with veins of quartz, chlorite, titanite and prehnite, muscovite – quartz – plagioclase mylonite schist, muscovite – chlorite – plagioclase schist, muscovite – biotite – chlorite – garnet schist, muscovite – chlorite – biotite – garnet – tourmaline schist, tourmaline – muscovite – rutile metaquartzite, and impure marble.

According to previous studies in the Baronie to the north (Fig. 1), the Monte'e Senes region reached the garnet–albite zone of Barrovian metamorphism during the late Variscan (Franceschelli *et al.* 1982). In addition to the occurrence of garnet and albite, maximum temperatures of the upper greenschist facies are indicated by annealed arcs of white mica around tight folds and by opening angles of quartz-*c* cross-girdles over the short principal axis *Z* of the strain ellipsoid (determined as the pole of the foliation plane; hence strain Z) of ~55° (Kruhl, unpubl. data).

The Variscan tectonic development north of Monte'e Senes has recently been studied (Helbing & Kruhl 2000). The similarity in the tectonic structures and their chronology between the area north of Monte'e Senes and those in the Monte'e Senes region suggests a similar development of both regions. During increasing metamorphism in the subgreenschist to lower greenschist facies, a foliation (S1) developed generally parallel to the sedimentary bedding. Numerous quartz veins formed parallel to S1, as is typical for metasedimentary rocks affected by a first deformation under increasing grade at greenschist-facies conditions. These veins may well survive later tectonic overprint and, thus, help to unravel the early stages of deformation history (Voll 1960, Nabholz & Voll 1963). Lineations (L1), together with rare shear-sense indicators, point to a top-to-the-southwest tectonic transport. A second episode of deformation (D2) probably started at the peak temperature and continued during decreasing temperatures. In the Monte'e Senes region, this episode is indicated by (i) S1 inclusion trails in garnet porphyroblasts, which are truncated by S2 white mica and biotite films outside the garnet and are subperpendicular to the general S2 trend, (ii) S2 wrapping around the porphyroblasts, (iii) equilibrated S1 white mica arcs between S2 crenulation cleavages, and (iv), locally, fine-grained (~20–30 μm) quartz due to recrystallization along S2 planes. Episode D2 led to isoclinal folds of S1-parallel quartz veins (F2) and a foliation S2 that is parallel to S1 in F2 limbs and to the sedimentary bedding, and appears as the main foliation in all rocks. The foliation S2 bears an east–west-oriented stretching lineation (L2). During a third deformation event (D3), S2 was folded around open to tight folds with axes invariably strictly parallel to F2. In the region north of Monte'e Senes, chloritization of biotite, fine-grained quartz recrystallization and brittle deformation of feldspar point to retrograde lower-greenschist-facies conditions during D3. The kinematic history ends with regional extension (D4) leading to locally numerous cm-spaced shear bands.

Intrusions of Felsic Magma: General Relationships

The Monte'e Senes complex covers an area of about 100 km^2 and provides a vertical section of up to 800 m. Numerous minor pulses of various felsic magmas intruded the schists prior to the intrusion of the main body of tonalite and formed sheets of felsic igneous rocks mostly parallel to the regional foliation of the country rocks. All intrusive rocks show evidence of solid-state flow, commonly superimposed on earlier magmatic flow. The geological map gives an impression of the broad tabular structure of the complex (Fig. 2). The strongly curved boundaries of the contacts reflect the intersection between the moderately inclined sheets of coarse-grained intrusive rock, the internal structures of which are not shown on the map, and the country rocks. The intrusive rocks have not been dated, but rocks of similar composition and geotectonic position in Sardinia have been dated at 302–307 and 289 Ma, respectively (Del Moro *et al.* 1975).

This intercalation of intrusive complex and country rock is reflected by the step-like morphology of the Monte'e Senes slopes (Fig. 3). The layering is moderately inclined to the southeast as a result of Eocene tilting. From the orientation of Mesozoic bedding north of Monte'e Senes, a Variscan subhorizontal position of the main foliation (S2) can be inferred (Kruhl, unpubl. data). Consequently, an originally subhorizontal position of the S2-parallel intrusive sheets is most likely. Nearly continuous outcrops along a road from below Monte'e Senes summit to the valley, covering a vertical distance of ~500 m, reveal the intimate interlayering of *ca.* 60 vol.% intrusive body and 40 vol.% country rocks (Fig. 4). The interlayering also occurs where the geo-

logical map shows continuous regions of either country rock or intrusive rock. This indicates the sheet-like character on the meter scale of more or less the entire intrusive body.

In addition to numerous centimeter- to decimeter-thick sheets of various felsic rocks, at least four different, more voluminous and widespread intrusive rock-types may be distinguished in the Monte'e Senes region, on the basis of their different composition and chronology. They occur as layers centimeters to several meters thick subparallel to the predominantly shallow layering and main foliation of the country rocks. Monte'e Senes shows an excellent section through the margin of the sheeted complex, with broadly conformable sheets of tonalite, which are discordant in detail. Some have apophyses. The sheets may contain microgranitoid enclaves and, locally, are crammed with small metasedimentary xenoliths, with their folia aligned parallel to the main foliation, and with quartz xenocrysts (presumably from dismembered quartz veins). The cross-cutting relationships and structures of these intrusive sheets may be studied in detail in a few outcrops along the road from Irgoli to Capo Comino, as well as near the summit of Monte'e Senes (Fig. 5), where a road section and several outcrops reveal details of the mode of intrusion and the relationship to regional deformation (Fig. 6).

On the basis of cross-cutting relationships, a chronological order of three different pulses of intrusion of tonalitic magma and the subsequent emplacement of leucogranitic material can be established (Fig. 6). The tonalitic sheets I + II are strongly foliated parallel to the regional S2, with a strong lineation (long axes of recrystallized biotite and feldspar aggregates) parallel to the regional L2. The main intrusive body of tonalite (III) is weakly foliated and shows a less intense lineation parallel to the regional L2. The foliation partly transects oblique apophyses and partly follows the borders of tonalite veins. Tonalite III cuts F3 folds and is itself transected by S4 shear bands. The intrusion of the leucogranitic magma postdates the D1 to D3 structures, but was deformed under low-temperature conditions (as shown below).

The indications of the intrusion of tonalitic magma forming during regional D2–D3 deformation, discussed in greater detail below, are supported by evidence that the tonalite shows microstructural indications of solid-state deformation superimposed on magmatic flow, and that the contact-metamorphic minerals show evidence of growth during deformation.

A few late, minor intrusive bodies cut the main tonalite at Monte'e Senes. The fact that they are also foliated and show evidence of solid-state deformation indicates that the regional deformation continued after the emplacement of the main tonalite.

Description of the Tonalitic Intrusive Bodies

Structures of intrusive pulses I – IV

The earliest intrusive pulses of the sequence gave rise to microtonalites that all have similar macro- and microstructures, pointing to a common history. However, microtonalite I contains more coarse-grained biotite, plagioclase and quartz phenocrysts. This, together with the same cross-cutting relationship in different outcrops, indicates that microtonalite I is the earlier and microtonalite II the later intrusive rock (Fig. 6). The microtonalitic rocks occur as cm- to m-thick layers parallel to S2 (Fig. 6). They have strong foliations parallel to the margins of the planar intrusive bodies and, therefore, parallel to the regional S2. The foliation contains an east–west lineation parallel to the regional D2 lineation (L2). The foliation is formed by a 100 μm- to mm-thin layering and the alignment of (i) lenticular biotite aggregates up to 5 mm long, (ii) quartz lenses up to 5 mm long, with an axial ratio of 2 to 3, (iii) euhedral phenocrysts and lenticular aggregates of plagioclase up to 2 cm long, and (iv) biotite, quartz and plagioclase grains in the groundmass 10–100 μm long (Fig. 7A).

Intrusive pulse III occurs as cm- to m-thick dykes parallel to the main foliation and layering of the country rocks, but locally with numerous branches cross-cutting the dykes of microtonalite I + II (Fig. 6). The microtonalite III dykes and locally even their cross-cutting branches are moderately foliated parallel to the country-rock foliation, indicating that at least part of the foliation formed by solid-state deformation. An east–west-oriented lineation occurs on the foliation planes, *i.e*., again parallel to L2 of the country rocks. The foliation is formed by aligned grains of igneous plagioclase and biotite. Locally, millimetric to centimetric spacing of S3 planes occur as μm-thick layers of white mica, along which the igneous plagioclase has been dissolved but not plastically deformed (Fig. 7F). However, on the outcrop scale, the dykes at least partly postdate the formation of D3 folds (Fig. 6). This timing may indicate (i) continuous emplacement of microtonalite III from D2 to the decline of D3 and (ii) a continuity of the kinematic framework from D2 to D3.

At several localities, leucogranite veins (intrusive pulse IV) cut the three tonalitic intrusive bodies as meter-thick sheets, with apophyses (Fig. 5A). Locally, the leucogranite is strongly foliated. but with only weakly elongate microgranitic enclaves. The foliation is formed by a weak alignment of cm-sized euhedral phenocrysts of K-feldspar. It is parallel to the margins of the sheets and, therefore, locally oblique to the foliation of the adjacent tonalites, indicating that the foliation of the leucogranitic sheets was mainly due to magmatic flow. However, microfabrics point to an additional component of solid-state deformation (see further below).

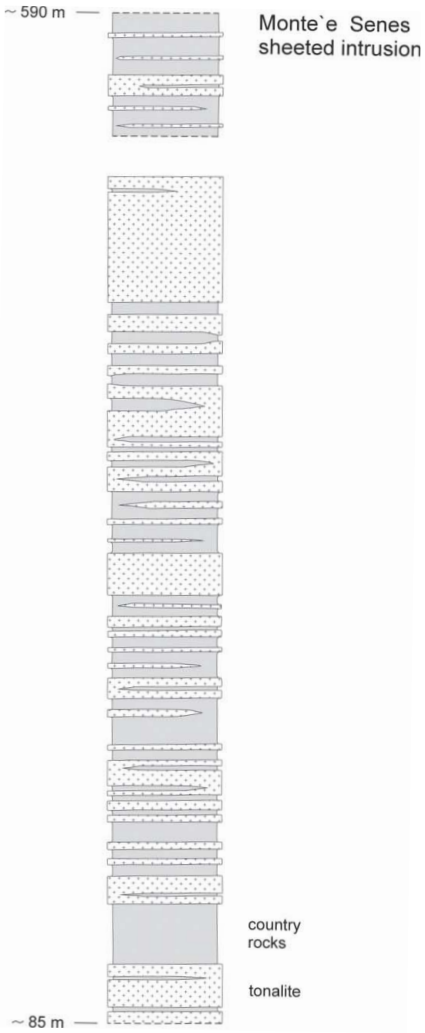

FIG. 3. Monte'e Senes viewed from the southwest. The sheeted intrusive bodies form light bands that are inclined toward the right (southeast) and can be seen as pronounced steps (arrows) along the northwestern slopes of the mountain.

Microstructures of intrusive pulses I – IV

The microtonalites I–II contain aggregates of biotite composed of numerous small strain-free grains, locally markedly oblique to the flat faces of the lenses (Fig. 7B). This attitude may be interpreted as the result of the recrystallization of former primary crystals of biotite. In tonalite III, biotite is locally altered to chlorite.

In the microtonalites I–II, the quartz lenses are former primary crystals, as indicated by their partly euhedral shapes with facets of roughly rhombohedral and prismatic orientations (Figs. 7A, C). They now contain a few large recrystallized grains of distinctly different crystallographic orientations and with strongly sutured grain-boundaries and mostly prismatic subgrain-boundaries. The axial ratios, *ca.* 1.5–2, suggest that the igneous crystals experienced only minor strain. The preferred *c*-axis orientations of recrystallized grains in these lenses, as well as of groundmass quartz, are weak cross-girdle patterns, symmetrical to the foliation and lineation, with an opening angle across strain *Z* of ~90°

FIG. 4. Semiquantitative profile (A–A' from Fig. 2) transferred to a 500-m vertical section showing the intimate interlayering of *ca.* 60 vol.% mainly tonalite-III intrusive bodies (crosses) and *ca.* 40 vol.% wallrocks (grey). Local interlayering on the decimeter scale is not resolved.

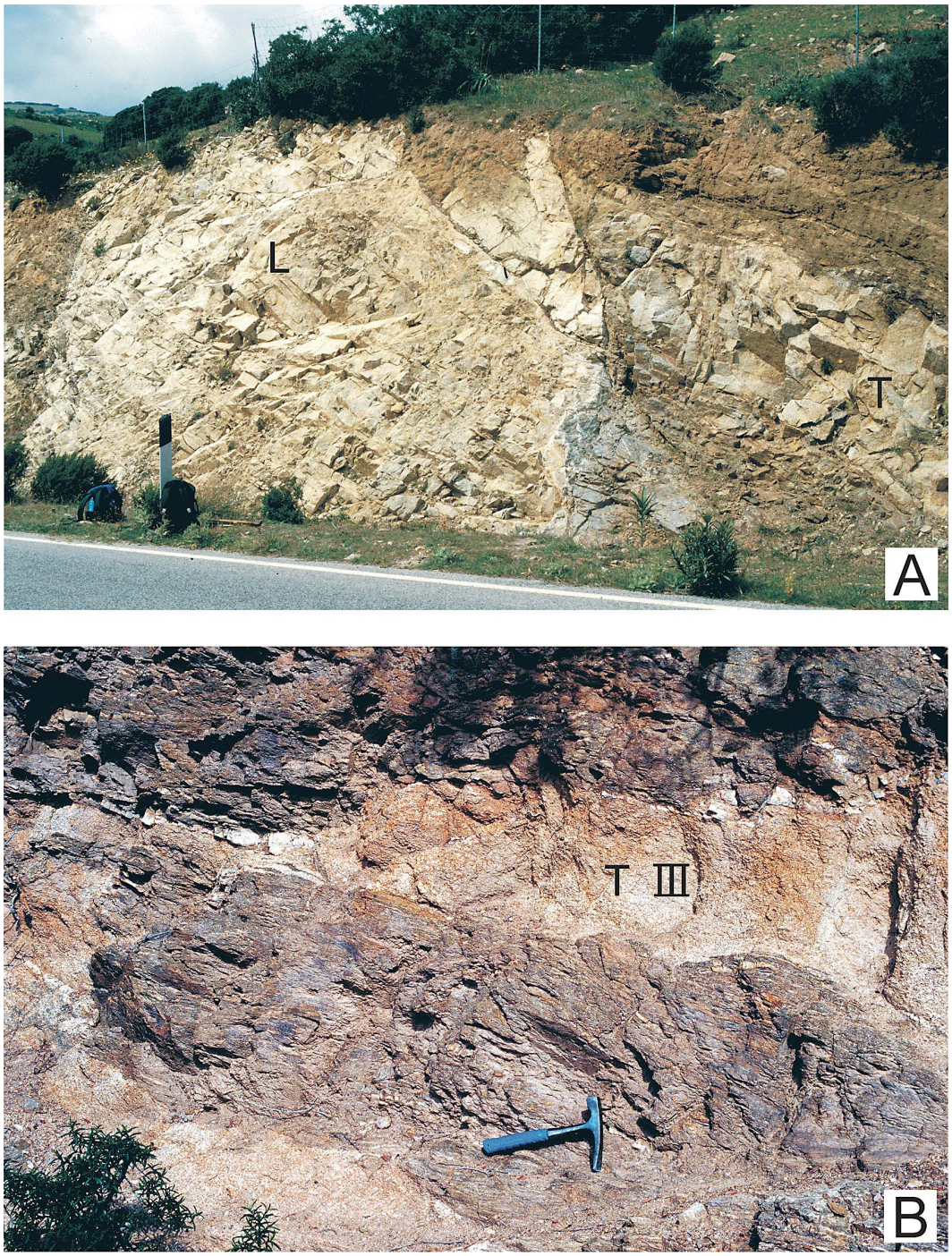

FIG. 5. A. A meter-thick sheet of tonalite (T) parallel to the southeast-dipping (*i.e.*, right) regional foliation and layering is cut by a subvertical intrusive body of leucogranite several meters thick (L); roadcut at the eastern margin of the Monte'e Senes intrusive body (locality 4569, road from Irgoli to Capo Comino; Fig. 2). B. Decimeter-thick intrusive body of tonalite-III (T III) subparallel to the well-foliated and thinly layered metapelitic contact-metamorphic wallrocks (locality 4576, southwest of Monte'e Senes summit; Fig. 2).

(Figs. 8A, B), but with additional maxima closer to strain *Z* for the recrystallized primary quartz. Intrusive pulse III shows quartz grains up to several mm across, with coarsely sutured grain-boundaries and strong chessboard patterns of subgrains (Fig. 7H), which indicate deformation in the stability field of high quartz (Kruhl 1996). The quartz is recrystallized along its margins to smaller grains, with only prismatic subgrain-boundaries, indicating deformation as low quartz. Deformation lamellae occur in the grains with strong prismatic subgrains. Locally, the parent quartz grains, which we infer to be of igneous origin, have been totally replaced by the new recrystallized grains, which may be up to *ca*. 1 mm across. The boundaries of the new grains are also sutured and locally recrystallized to grains 10–100 μm across.

The euhedral, platy, mm-sized crystals of igneous plagioclase, aligned in the microtonalite I–II foliation, have axial ratios of 3 to 4 (Fig. 7D). Their partly saussuritized cores ($An_{45–55}$ in fresh parts) are mantled by a rim up to 300 μm thick (*ca*. An_{35}), which overgrows the aligned grains in the groundmass (mainly biotite) (Fig. 7E). The igneous grains are partly replaced by equidimensional "clear" grains (Fig. 7F), with compositions of $An_{40–45}$, which we interpret as recrystallized grains. The plagioclase lenses in the same rocks have axial ratios of 1 to 3. Their outlines partly show a subhedral shape, with faces parallel to (010) and locally parallel to (110) (Fig. 7A). The lenses are composed of several polygonal grains with diameters of 200–300 μm and grain-boundary facets that are not preferentially oriented parallel to low-index planes (Fig. 7B). Their compositions are $An_{40–45}$. Multiple deformation twins ~5 μm across, after the albite and pericline laws, are locally developed. The grains show a crystallographic preferred orientation, with (010) roughly parallel to the foliation, [100] in the foliation and subperpendicular to the lineation, and (001) partly subparallel to the foliation, as well as subperpendicular to the lineation (Fig. 9A). These observations suggest that the plagioclase lenses represent former igneous crystals that recrystallized during the solid-state deformation of the rock.

On the other hand, in the plagioclase-rich layers, the plagioclase grains are euhedral to subhedral and have a preferred orientation according to shape, as well as a crystallographic preferred orientation, with (010) strongly aligned in the foliation and a broad [100] maximum near the lineation (Fig. 9B). This type of preferred orientation is regarded as typical of meta-igneous rocks (Shelley 1993, p. 358). In the plagioclase-rich layers, the dihedral angles at triple junctions are far from minimum-energy values. These observations argue against recrystallization, and instead for an igneous-flow-induced structure of the layers or for preferred growth of crystals in a stress field.

In microtonalite III, grains of igneous plagioclase are commonly several mm long. Some of them are partly or totally replaced by large, polygonal, equidimensional grains, *ca.* 500–700 μm across (Fig. 7H), with similar crystallographic orientation, which we interpret as recrystallized grains. The igneous grains are fractured and kinked, and locally, new K-feldspar has grown between the fragments. Igneous and recrystallized grains show thin lamellar deformation-induced twins after the albite and pericline laws.

The foliation in the groundmass of tonalites I and II, formed by aligned small grains of biotite and plagioclase, is not distorted around the mm-size euhedral phenocrysts of igneous plagioclase (Figs. 7D, E). Rarely, weak "pressure shadows" are developed. These relationships indicate only a weak component of solid-state deformation after the crystallization of the tonalite.

In the intrusive pulse IV (leucogranite), the K-feldspar is mainly microcline (simply twinned and finely perthitic) and contains rectangular inclusions of plagioclase, as is common in phenocrysts of K-feldspar in granites (*e.g.*, Vernon 1986). The microcline has been locally partly replaced by myrmekite and muscovite as a result of hydration during deformation (Ashworth 1972, Phillips *et al.* 1972). Rounded inclusions of quartz are common in the microcline, especially in the outer parts of the microcline phenocrysts. The inclusions have been formed by solid-state modification of granophyric intergrowths, which suggests that this is a high-level intrusive body.

The Contact Aureole

Minerals in the contact-metamorphosed schists and their textures

The contact zones show numerous conformable sheets of foliated tonalite (transgressive in detail) and various felsic rocks, all of which have been strongly deformed and which predate the main intrusive body (tonalite III), interlayered and interfingered with sillimanite schist containing dismembered quartz veins and small quartzofeldspathic veins. The microfabrics in the contact-metamorphic aureole of the main intrusive body indicate a long-lasting and partly synchronous history of deformation and intrusion.

The main minerals in the schists near the contact are quartz, biotite, muscovite, cordierite, andalusite and sillimanite. The metapelitic layers are rich in biotite, with locally abundant andalusite, locally abundant fibrous sillimanite, less common prismatic sillimanite, and much less abundant quartz. Corundum occurs in quartz-poor areas. The metapsammitic layers (presumably beds) consist of quartz, with dispersed biotite and muscovite, with or without dispersed cordierite and sillimanite, especially in more strongly deformed rocks.

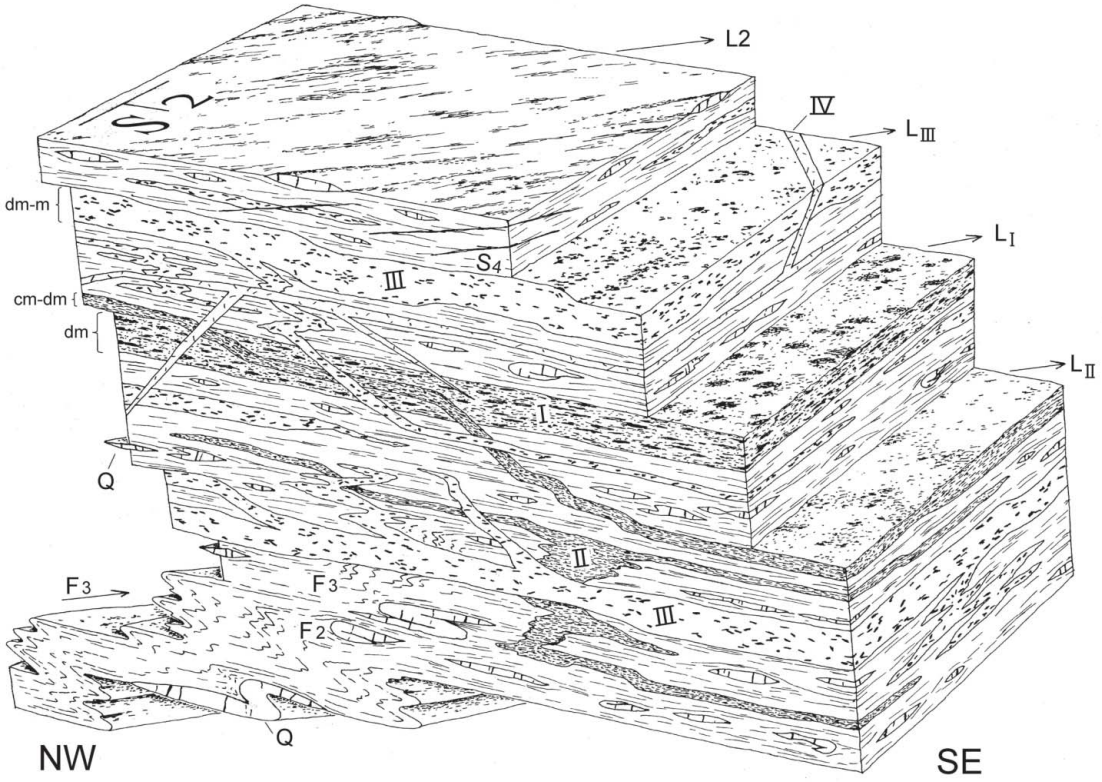

FIG. 6. Schematic sketch of intrusive body and deformation relationships from outcrops 4569 and 4576, partly shown in Figure 5, showing a chronological sequence of three intrusions of tonalitic magma, a subsequent intrusion of leucogranitic magma, represented by a vein net, and the structures of the regional deformations D2, D3 and D4, with foliations S, lineations L and fold axes F. Q represents S1-parallel quartz veins.

FIG. 7. Photomicrographs of deformation fabrics in the intrusive bodies. Crossed polars. (A) Tonalite I: aggregates of recrystallized grains of igneous plagioclase (P), biotite (B) and quartz (Q); outlines emphasized by broken lines. The box outlines figure B. Sample 4569M; section perpendicular to the foliation and parallel to the lineation; long side (LS) of the photomicrograph: 7 mm. (B) Tonalite I: detail of figure A; lenses of recrystallized igneous plagioclase (P), with polygonal recrystallized grains and biotite (B), with recrystallized grains partly oblique to the flat face of the former igneous grain; LS: 3.1 mm. (C) Tonalite I: coarsely recrystallized igneous quartz with the flat face parallel to recrystallized biotite flakes (former igneous grains) that form the strong foliation. Sample 4569A; section perpendicular to the foliation and parallel to the lineation; LS: 3 mm. (D) Tonalite II: platy euhedral plagioclase in a finer-grained groundmass of elongate quartz, plagioclase and biotite grains. The flat faces of all these grains form a strong foliation. Sample 4569B; LS: 7 mm. (E) Tonalite I: igneous plagioclase phenocryst with a saussuritized core (c) (*ca.* An_{50}) and a rim (r) (*ca.* An_{30}), which overgrows aligned biotite of the groundmass. The phenocryst is aligned parallel to the foliation formed by the flat faces of groundmass biotite, quartz and plagioclase; sample 4569A; section perpendicular to the foliation and parallel to the lineation; gypsum test plate; LS: 3.1 mm. (F) Tonalite I: igneous plagioclase with albite growth-twins (P1 and P2), partly replaced by smaller equant, "clear" grains (r), again with albite growth-twins; sample 4569A; LS: 1 mm. (G) Tonalite III: pressure solution of igneous plagioclase grains along S3 films of white mica. The compositional zoning of the plagioclase is cut by S3. Sample 4569L; LS: 3.1 mm. (H) Tonalite III: large grain of quartz with prismatic (p) and basal (b) subgrain ("chessboard") pattern; aggregate of recrystallized plagioclase (r); sample 4575F; LS: 3.1 mm.

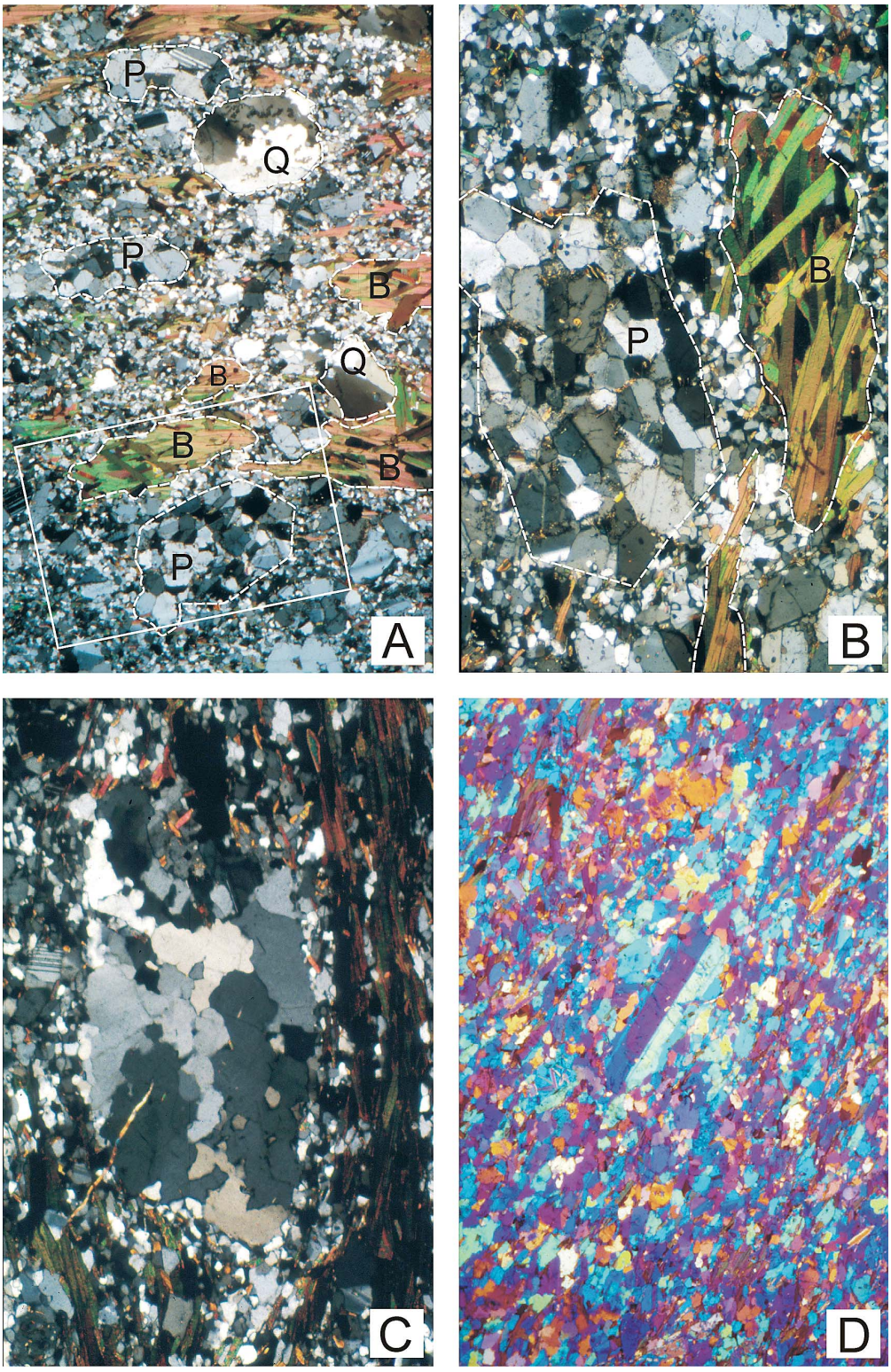
P
Q
P
B
Q
B
B
B
P
A
B
P
B
C
D

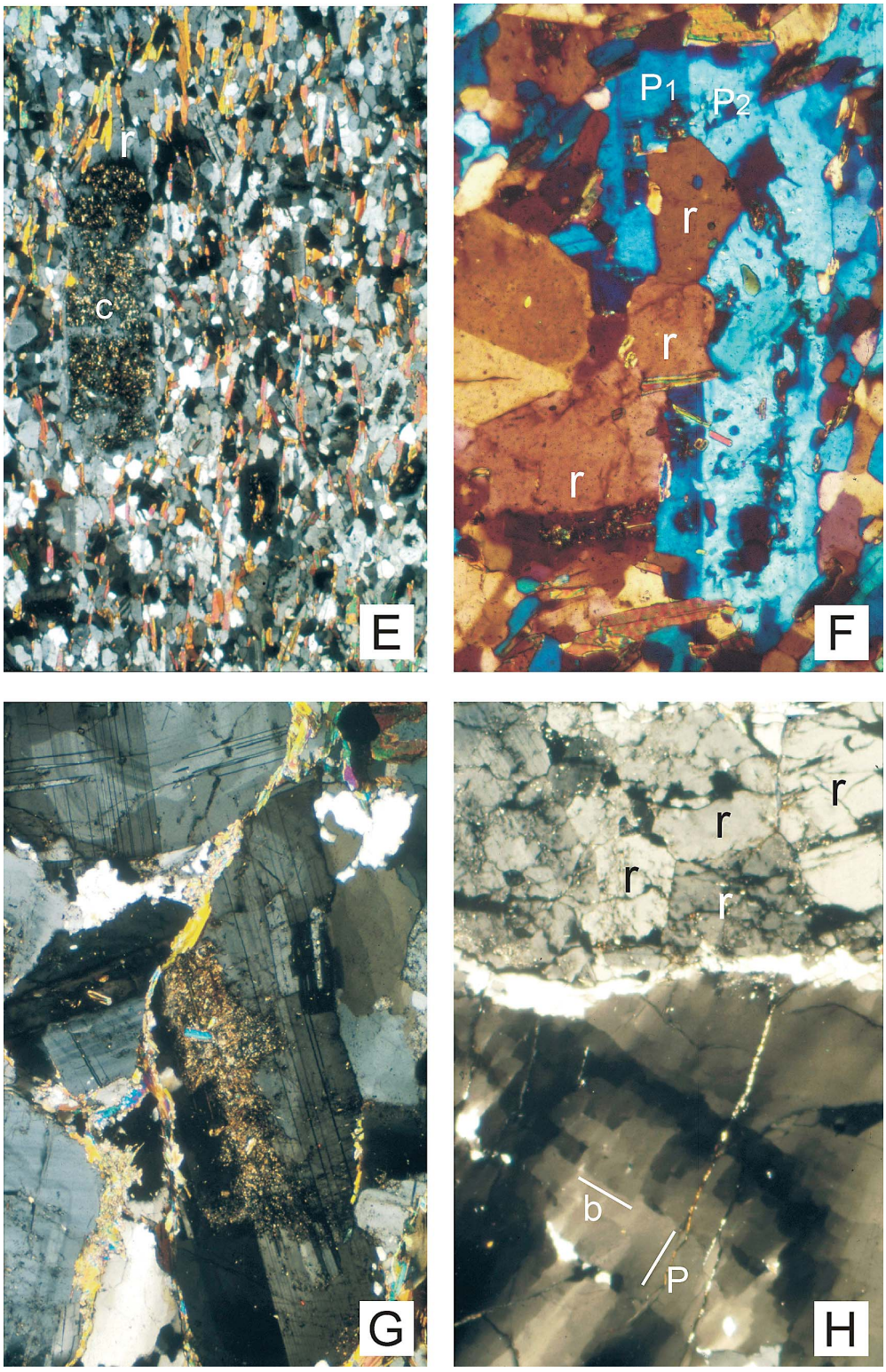
r
c
E
P1
P2
r
r
r
F
G
r
r
r
r
b
P
H

Biotite is the most abundant mineral in the metapelitic layers of these schists; it occurs as decussate aggregates that preserve the geometry of the main foliation, though many grains are oblique to it. In some rocks, biotite (with sillimanite; see below) occurs in new folia oblique to the main foliation. In places, this may be a crenulation parallel to the main foliation, suggesting that the main foliation was formed as a crenulation cleavage. In other places, it is a crude crenulation parallel to the axial surfaces of folds that deform the main foliation, bedding and veins, and, on the basis of macrostructures, are interpreted as D3 folds. The biotite is pleochroic in shades of brown, and contains numerous pleochroic haloes. Alteration to chlorite is rare and local.

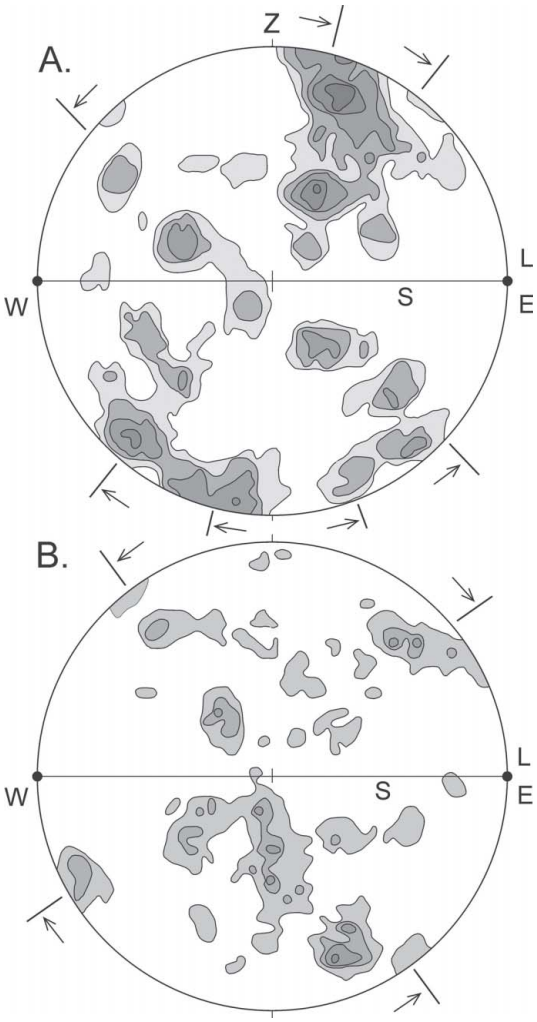

FIG. 8. Preferred quartz *c*-axis orientations; universal-stage measurements, equal-area projection, lower hemisphere; S: foliation plane, L: east–west-oriented lineation (L2) (filled circle); Z: short axis of strain ellipsoid, assumed perpendicular to S. (A) Tonalite I: sample 4569A; 231 *c*-axes from recrystallized igneous grains; contouring: 1.0 times uniform distribution, starting with 1.0. (B) Tonalite II: sample 4569B; 300 *c*-axes from groundmass grains; contouring: 0.8, starting with 1.6.

In quartzofeldspathic and quartz veins in the contact zone, coarse-grained quartz is elongate in the foliation and shows a weak chessboard pattern of subgrains, indicating temperatures of at least 620–650°C during deformation of the veins, with a presumed minimum pressure of *ca.* 200–300 MPa. It encloses S2-parallel trails of fibrous sillimanite, biotite and cordierite. This texture suggests grain coarsening and at least weak deformation in the stability field of high quartz (Kruhl 1996) after formation of S2. Locally, the elongate grains of quartz are folded around open to tight D3 folds on the cm–dm scale, with flatly west-dipping axes. The folds have an axial-plane-parallel foliation formed by bands of fibrous sillimanite and aligned biotite and quartz. The quartz grains aligned in S3 do not show a chessboard pattern of subgrains, but only prismatic subgrain-boundaries. We interpret this as indicating a lower temperature during D3.

Sillimanite is variably distributed, but is locally abundant in the metapelitic layers, where it may define the main foliation, with biotite. Commonly, it occurs in ragged fine-grained, fibrous aggregates, many of which show local microfolding, and is intergrown with biotite. Though most of the sillimanite is fine-grained and fibrous, larger prismatic grains are present in places, and idioblastic prismatic crystals may occur in contact with fine-grained, fibrous aggregates; both are inferred to be compatible members of the same assemblage (*e.g.*, Vernon 1975). Mostly the sillimanite occurs with biotite and quartz, without andalusite. However, some prismatic sillimanite has replaced andalusite coaxially (*e.g.*, Bosworth 1910, Vernon 1987a), and occurs as parallel prisms or, alternatively, arms of a prismatic sillimanite dendrite that are connected in three dimensions. Locally, aggregates of parallel and subparallel fibers of sillimanite appear to have partly replaced andalusite.

Fibrous sillimanite occurs locally as concentrations along grain boundaries of most of the other minerals, including biotite, andalusite and quartz, forming radiating "sprays" of fibers projecting into (*i.e.*, replacing) these minerals (Fig. 10A). It forms thin layers along quartz–quartz and quartz–cordierite boundaries, parallel to the D2 foliation (S2), which has been folded around open D3 folds (F3), as well as parallel to the foliation (S3) related to F3. These observations point to a period of sillimanite growth that started pre-D2 and was still active during D3. Sillimanite does not occur along sutured grain-boundaries (Fig. 10D).

Spectacular "sprays" of fibrous sillimanite have replaced and project out from cordierite in some quartz-rich layers (Fig. 10B). These occurrences of fibrous

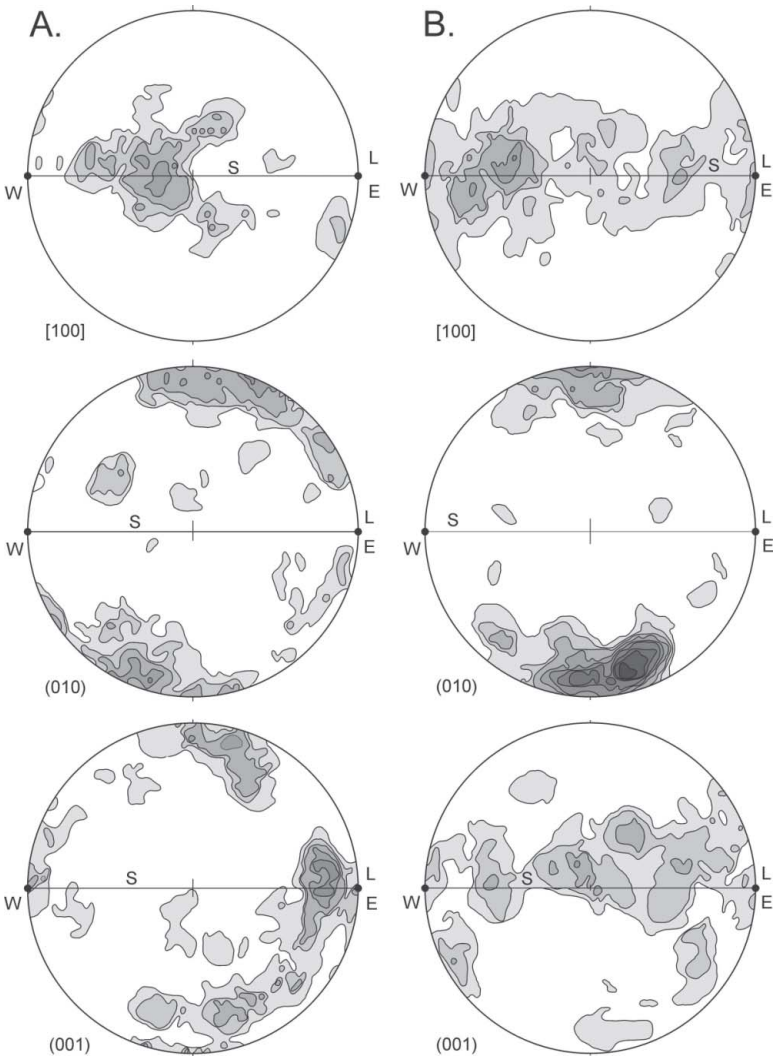

FIG. 9. Plagioclase: preferred orientations of crystallographic planes and directions; universal-stage measurements, equal-area projection; S: foliation plane, L: east–west-oriented lineation (filled circle). (A) Tonalite I (sample 4569A), recrystallized igneous grains: 144 (001) and 187 (010) and [100] measurements; lower hemisphere, contouring: 0.6 times uniform distribution, starting with 1.8. (B) Tonalite II (sample 4569B), groundmass grains: 121 (001) and 127 (010) and [100] measurements; lower hemisphere, contouring: uniform distribution, starting with 1.0.

sillimanite are similar to the fibrous sillimanite at Cooma, southeastern Australia, which has been interpreted as resulting from base-cation leaching (hydrogen metasomatism) by acid solutions, probably in the stability field of sillimanite (Vernon 1979). Folia rich in fibrous sillimanite also delineate domains in a locally developed crenulation cleavage (Fig. 10C), as do folia of biotite (Vernon 1987b).

Cordierite occurs in the quartz-rich beds, but is absent from the metapelitic beds. It forms small, dispersed, xenoblastic grains, mostly altered to fine-grained chlorite and micaceous aggregates; it rarely shows crystal faces against the quartz. The cordierite encloses small (~100 μm) rounded quartz grains (Fig. 10B) and, together with biotite, is enclosed in coarsely sutured quartz grains, and pins the grain-boundary sutures (Fig. 10D).

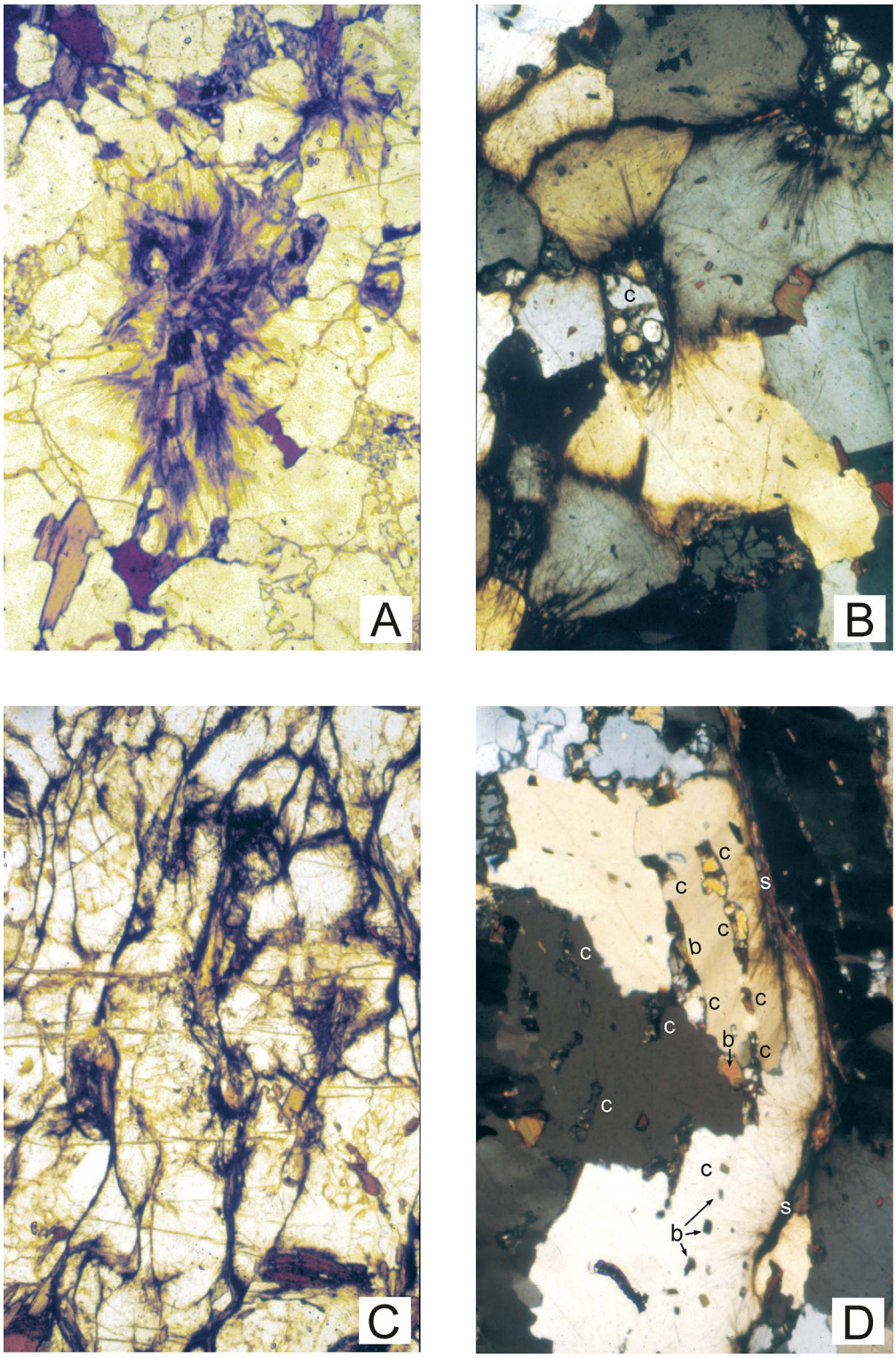
A
B
c
C
D
c
c
s
c
c
b
c
c
c
c
b
c
c
c
b
s

In S2-parallel quartz veins, the cordierite grains are elongate parallel to S2 (Fig. 10D). The coarsening and suturing of quartz thus occurred subsequently to the alignment of the minerals and formation of S2. The coarse-grained quartz has a weak chessboard pattern of subgrains and is folded around open D3 folds. These observations suggest that growth of cordierite started in the early stage of contact metamorphism, in still fine-grained host rocks, during or even prior to D2, and was at least partly outlasted by D2 and D3.

Andalusite occurs as large, irregularly shaped grains and scarce idioblasts, in symplectitic intergrowths with quartz, and in intergrowths with biotite in the metapelitic layers. Coarse-grained andalusite encloses rounded grains of corundum in quartz-free areas, as well as aligned grains of biotite much smaller in size than outside the andalusite. The andalusite recrystallized and developed subgrain patterns and grain-boundary sutures.

Muscovite is less abundant than biotite (except in schists showing evidence of retrograde metamorphism). It occurs in the metapelitic layers, as grains intergrown with biotite in decussate aggregates, without evidence of replacement and therefore apparently as a member of the main compatible mineral assemblage. This assemblage included biotite and andalusite, and probably muscovite also coexisted with the later-formed sillimanite. Some of the intergrown grains of muscovite are much larger than the average grains of biotite, and are oblique to the main foliation. Nevertheless, they are intergrown with biotite, without evidence of incompatibility. Therefore, we have no clear evidence that these oblique grains formed later than the other muscovite grains in the metapelitic layers. However, some of the coarse-grained muscovite contains folded trails of inclusions of fibrous sillimanite, suggesting a relatively late origin for this muscovite, although this need not imply a later origin for all the muscovite in the rock.

FIG. 10. Photomicrographs of microstructures in the contact aureole. Crossed polars if not indicated otherwise. (A) Fibrous sillimanite spraying into quartz of a quartz-rich layer. Sample 4575A; parallel polars; long side (LS) of photomicrograph is 3.1 mm. (B) Residual cordierite (c) with rounded quartz inclusions in a quartz-rich layer. Fibrous sillimanite along grain boundaries sprays into quartz and cordierite. Sample 4576A; LS: 3.1 mm. (C) Fibrous sillimanite anastomosing veins through quartz, feldspar, muscovite, and biotite. Sample 4574; parallel polars; LS: 3.1 mm. (D) Cordierite (c) and prismatic sillimanite (s) aligned in S2 and gently folded about F3. Fibrous sillimanite sprays from S2 away into neighboring coarsely sutured grains of quartz, which partly overgrow S2-aligned cordierite, sillimanite and biotite (b) and are partly pinned by these grains. Sample 4576A; LS: 3.1 mm.

Also, locally the contact-metamorphosed schists show evidence of extensive replacement of andalusite and sillimanite by late muscovite. The inferred late muscovite may have formed in response to declining temperature, but alternatively, it could have been due to changes in the activity of H_2O, the activity of potassium ions or the pH of the reacting system (*e.g.*, Eugster 1970, Wintsch 1975, Vernon 1979). For example, it could have been controlled by hydrous solutions formed during the later stages of cooling of the main tonalitic magma. With so many potential controlling variables, muscovite could have had a long, complex and indecipherable growth-history in these rocks.

Quartz-rich veins in the contact-metamorphosed schists

Folded quartz-rich veins and disrupted beds of metaquartzite are common in the contact-metamorphosed schists. They consist of varying proportions of quartz, plagioclase (partly replaced by white mica), biotite and muscovite, with or without fibrous sillimanite or altered cordierite. The veins appear to have been inherited from the parent rocks, as similar quartz-rich veins are abundant in low-grade schists away from the contact. The quartz in the veins and deformed beds is deformed, commonly with prismatic subgrain-boundaries (indicating low-temperature *a*-slip), but locally showing basal subgrain-boundaries (indicating higher-temperature *c*-slip) as well. Some of the quartz shows strain-induced grain-boundary migration.

Some folded quartz-rich veins are cut by a new axial-surface foliation consisting of muscovite and biotite or fibrous sillimanite. Many fibrous aggregates of sillimanite spray out from the sillimanite folia and pods. Sillimanite also occurs as sprays of radiating fibers projecting from vein-like concentrations of fibrous sillimanite along the quartz, biotite and cordierite grain-boundaries, forming an anastomosing foliation parallel to the main foliation and the new axial-surface foliation. The sillimanite aggregates were initially concentrated in existing grain-boundaries, but gradually became more continuous and vein-like in selected channels parallel to the new axial-surface foliation, locally stepping across to the main foliation; the result is an irregular, wavy foliation.

In other disrupted quartz-rich beds, cordierite has been preferentially replaced by fibrous sillimanite, leaving the original inclusions of rounded quartz in the cordierite as remnants in the pseudomorphs. The sillimanite commonly "sprays" out into the surrounding quartz, muscovite and biotite. In places, it appears that quartz–quartz grain boundaries are affected by the sillimanite fibers, but not in other places. This may imply that quartz recrystallization accompanied or postdated the growth of sillimanite in some places, but not in others. We suggest that cation leaching has been involved

in forming the sillimanite concentrations, as mentioned previously.

Quartzofeldspathic veins in the contact-metamorphosed schists

Small deformed quartzofeldspathic veins, in places resembling leucosome in migmatites, occur in some of the contact-metamorphic schists. As discussed later, the temperatures may have been too low for melting. If so, the veins are injections, and the rocks may be called "injection migmatites". The source could have been any of the earlier felsic intrusive pulses or the main granitic magma, but because the veins are rich in plagioclase, they probably come from the main tonalitic magma.

The felsic veins consist of recrystallized quartz, plagioclase and muscovite, with less abundant biotite and local elongate patches and radiating aggregates of fibrous sillimanite. As explained in the discussion, we interpret the sillimanite as being metasomatic, rather than indicating precipitation from a local peraluminous crustal melt. Muscovite varies from minor to locally abundant and is coarse grained. Some of the muscovite is in symplectitic intergrowths with quartz.

The plagioclase is oligoclase–andesine, and shows patchy zoning from a more sodic core to a more calcic rim. The plagioclase consists of (1) large grains showing some zoning, which presumably crystallized from the magma, and (2) small irregularly shaped aggregates of myrmekite, which grew in the solid state and which are commonly intergrown with muscovite. The aggregates appear to have replaced larger grains. No residual K-feldspar has been observed, and so we cannot be sure of the myrmekite-producing reaction, but arguing by analogy with most myrmekite elsewhere and from evidence in some of the larger leucogranitic sheets (see below), the myrmekite in the felsic veins may have replaced magmatic K-feldspar that occurred in irregular grains. The fact that both types of plagioclase occur in the same rock also suggests that the myrmekitic variety was formed in a different way from the zoned plagioclase. The larger grains of plagioclase are not myrmekitic, though some have a myrmekitic margin, which is consistent with nucleation of the myrmekite on existing plagioclase; this is typical of myrmekite replacing K-feldspar in deformed granitic rocks (*e.g.*, Phillips 1974, 1980, Vernon 1991). Presumably the K-feldspar grains were so small that the replacement was complete, in contrast to the larger sheets of leucogranite, in which the replacement was restricted to grain margins. The myrmekite seems to have been accompanied by the development of late muscovite (*e.g.*, Ashworth 1972, Phillips *et al.* 1972), and so may have been due to of a set of related reactions that resulted from introduction of H_2O late in the history of the veins. This interpretation is consistent with the evidence of late muscovite in the metapelites (Vernon 1979), as discussed below.

The quartz in the deformed quartzofeldspathic veins has a well-developed chessboard pattern of subgrains, reflecting high-temperature deformation. In folded quartzofeldspathic veins, discontinuous patches and lenses of fibrous sillimanite may define a new foliation, continuous with a new foliation in the adjacent schist.

Discussion

Metamorphic grade of the contact-metamorphosed schists

On the basis of thin-section observations, as well as staining of sample slabs, no K-feldspar has been observed in the contact-metamorphosed schists, and possible pseudomorphs of K-feldspar have not been observed. Peak conditions of metamorphism thus did not exceed those of the upper hornblende hornfels facies, having entered the stability field of sillimanite, but without having crossed the muscovite + quartz breakdown reaction. On the other hand, quartz in the contact-metamorphosed schists shows a chessboard pattern of subgrains and, therefore, is considered to have been deformed in the stability field of high quartz (Kruhl 1996), which starts at higher temperatures than the muscovite + quartz breakdown reaction. Therefore, most of the muscovite was formed during retrograde metamorphism. This is in agreement with the observation of corroded relics of andalusite, cordierite, prismatic sillimanite and corundum in single grains of muscovite, as well as locally abundant replacement of fibrous sillimanite by muscovite aggregates.

The relative time of formation of cordierite and andalusite cannot be determined; they could have formed simultaneously, together with biotite, in the prograde reaction: Ms + Chl + Qtz = Crd + And + Bt + V (Pattison & Tracy 1991, p. 132). The contact-metamorphic aureole is an example of a facies series 2a sequence of Pattison & Tracy (1991). The inferred P–T conditions, based on the triple point of Pattison (1992), are illustrated in Figure 11. The shaded area represents the stability field of the assemblage Ms + Crd + Als + Bt + Qtz, and shows the isopleth for biotite Mg/(Mg + Fe) = 0.5 (Pattison *et al.* 2002, Fig. 10). The assemblage indicates a pressure range of 300–400 MPa, namely between point X (appearance of Sil below reaction 3) and point Y (upper stability-limit of And + Bt). The pressure range would be ~200–300 MPa based on the triple point of Holdaway (Pattison *et al.* 2002, Fig. 10).

The sillimanite schist of the contact zones contains dismembered quartz veins and small quartzofeldspathic veins. The peak temperature of metamorphism may have been too low for partial melting, assuming that our inference that the rocks belong to a facies series 2a se-

quence of Pattison & Tracy (1991) is correct. In this situation, the reaction Ms + Qtz = Als + Kfs + V occurs at lower temperatures than the granite minimum melting curve (Pattison *et al.* 2002, Fig. 10), as shown in Figure 11. Therefore, the presence of the assemblage And or Sil + Ms + Qtz and the absence of K-feldspar indicate that the temperature of the Ms + Qtz breakdown reaction was not reached. If so, the quartzofeldspathic veins must have been injected into the schists.

Locally in the contact-metamorphosed schists, aggregates of parallel and subparallel fibers of sillimanite appear to have partly replaced andalusite. Therefore, we interpret the sillimanite as having resulted from a progression from the andalusite to the sillimanite field of stability, which was most probably due to increasing temperature. In general, pressure increase would be also possible, but the contact-metamorphic setting does not suggest such an increase. If the sillimanite grew in its P–T field of stability, the andalusite must have persisted metastably.

Microstructural evidence of deformation during contact metamorphism

Much of the sillimanite occurs in radiating aggregates, and much of the biotite and muscovite are in decussate aggregates, rather than in well-aligned folia, suggesting that the post-intrusive low-T deformation occurred only locally. The heat for the metamorphism probably came from the main tonalite (intrusive pulse III), rather than the earlier pulses, which have been strongly deformed and recrystallized, although they may have begun the heating of the aureole rocks, as discussed below. However, though the contact-metamorphic rocks do not appear to be strongly deformed, they show microstructural evidence indicating that some deformation accompanied the contact metamorphism, as follows.

(1) Sillimanite forms thin layers along quartz–quartz and quartz–cordierite boundaries, parallel to the D2 foliation (S2), which has been folded around open D3 folds (F3), as well as parallel to the foliation (S3) related to F3. But it does not occur along sutured grain-boundaries (Fig. 10D). These observations point to a period of sillimanite growth that started prior to D2 and was still active during D3.

(2) Pinning of quartz grain-boundary sutures by enclosed, S2-parallel cordierite indicates coarsening and suturing of quartz after the formation of S2. The coarse-grained quartz has a weak chessboard pattern of subgrains and is folded around open D3 folds. These observations suggest that growth of cordierite started in the early stage of contact metamorphism, in still fine-grained host-rocks, during or even prior to D2, and was at least partly outlasted by D2 and D3.

(3) The growth of andalusite also appears to have been syn-deformation. Coarse-grained andalusite encloses aligned grains of biotite much smaller in grain size than outside the andalusite. Andalusite recrystallized and developed subgrain patterns and grain-boundary sutures. It has been replaced by fibrous and prismatic sillimanite.

(4) Microfolds in sillimanite-rich aggregates in some metapelitic layers show individual bent and kinked grains of sillimanite, as well as undeformed prismatic grains of sillimanite transgressing the folded foliation, which suggest that sillimanite continued to grow after deformation of earlier-formed sillimanite.

(5) New folia parallel to the axial surfaces of small (probably D3) folds of bedding, veins and the main (D2) foliation are delineated by the highest-grade metamorphic minerals, especially fibrous sillimanite. In places, this sillimanite has been replaced by fine-grained muscovite, presumably after the deformation. Because the sillimanite folia cross quartz-rich layers or veins, the necessary chemical components for sillimanite must have been introduced on the local scale.

(6) In the deformed quartz-rich veins and quartzofeldspathic veins, quartz commonly has a chessboard pattern of subgrains, owing to the presence of prismatic and basal subgrains. They indicate deformation and re-

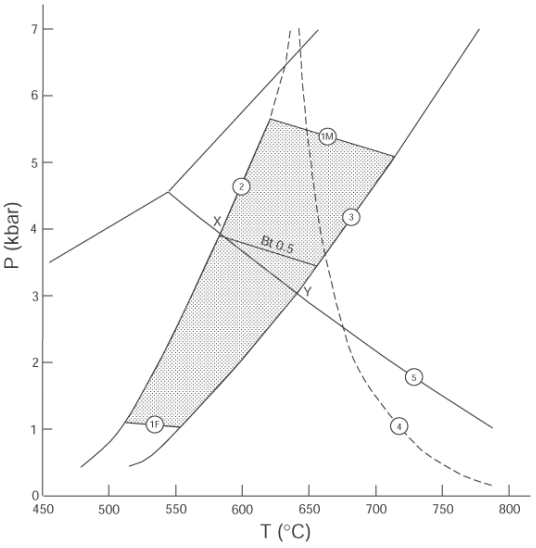

FIG. 11. Calculated phase-equilibria (after Pattison *et al.* 2002, Fig. 10) relevant to the Monte'e Senes rocks, showing the aluminosilicate curves (5) of Pattison (1992), the "wet granite" melting curve (4), and the reactions: Ms + Crd = Bt + Als + Qtz + H_2O (1M = Mg system; 1F = Fe system), Ms + Chl + Qtz = Crd + Als + Bt + H_2O (2), and Ms + Qtz = Kfs + Als + H_2O (3). The shaded area represents the stability field of the assemblage: Ms + Crd + Als + Bt + Qtz, and shows the Mg/(Mg + Fe) = 0.5 isopleth for biotite (Pattison *et al.* 2002, Fig. 10).

covery at temperatures of *ca.* 620–670°C as a minimum, on the basis of 200–400 MPa pressure (Kruhl 1996).

Microstructural evidence of the syntectonic nature of the intrusive rocks

In addition to the microfabrics of the contact-metamorphosed country-rocks (described above), the microfabrics of the intrusive rocks provide indications of their syntectonic nature and details of their deformation history. Because the temperatures of regional metamorphism did not exceed temperatures of the upper greenschist facies (<500°C; described above), any deformation at a higher temperature has to be related to the heat of the intrusive bodies themselves. Taking into account that (i) the intrusion spanned D2 to post-D3 and (ii) the temperature maximum of regional metamorphism was reached before or during D2, as inferred from studies in the Baronie area north of Monte'e Senes (Francescelli *et al.* 1989, Helbing & Kruhl 2000) and in the Nurra area, northwestern Sardinia (Carmignani et al. 1980, Francescelli *et al*. 1989, Volland 1999), the Monte'e Senes magmas were probably injected during regional uplift and cooling.

Microtonalites I and II were sheared during intrusion, crystallization and high-temperature subsolidus conditions during D2, as supported by the following points of evidence.

(1) A strong alignment due to magmatic flow, indicated by (i) shape orientation of biotite and plagioclase phenocrysts, and (ii) crystallographic preferred orientation of euhedral groundmass plagioclase is geometrically related to the D2 foliation and lineation. In other words, the D2 foliation was already present to guide flow of the magma.

(2) The igneous quartz phenocrysts are recrystallized to a few grains with coarse grain-boundary sutures and a crystallographic preferred orientation of *c* axes geometrically related to D2 and L2. The opening angle of the cross-girdle pattern across strain *Z* of ~90° is known from granulite-facies rocks (Sander 1930, Lister & Dornsiepen 1982) and is in agreement with deformation temperatures of ~700–750°C (Kruhl 1998).

(3) The groundmass quartz shows a similar crystallographic preferred orientation.

(4) The igneous plagioclase phenocrysts are partly recrystallized to polygonal grains of 200–300 μm across with compositions of $An_{40–45}$, *i.e.*, similar to that of the phenocrysts. The recrystallized grains show crystallographic preferred orientations, with (001) subparallel to S2 and subperpendicular to L2 and with [100] subperpendicular to L2. Such plagioclase orientations, with (001) concentrations parallel to the foliation and variable [100] maxima in the foliation, have been reported from amphibolite- to granulite-facies rocks (Kruhl 1987, Ji & Mainprice 1988, Kruhl & Huntemann 1991, Rosenberg & Stünitz 2003). Moreover, the grain size of the recrystallized polygonal grains, 200–300 μm, is in agreement with temperatures of ~600°C (Kruhl 2001).

All the solid-state deformation occurred at temperatures well above the maximum temperature of regional metamorphism and, therefore, is related to the heat of the cooling bodies of tonalite I and II. Indications of lower-temperature deformation, at lower-amphibolite- and greenschist-facies conditions, are rare.

The following two questions concerning the deformation have to be addressed. (1) Why are features of low-T deformation rare and features of high-T common? We infer that this is due to the rapid rate of cooling of the small bodies of tonalite, in combination with the weak stress-field during intrusion. Such a "gap" in the occurrence of high- and low-temperature deformation structures has been observed in other syntectonic intrusive bodies (Miller & Paterson 1994). The low differential stress is indicated by the low strain of the recrystallized quartz and aggregates of plagioclase grains and by their weak crystallographic preferred orientations. (2) Why were the quartz and plagioclase phenocrysts plastically deformed and recrystallized at high temperatures, whereas the groundmass grains were not? One reason may be that the groundmass was still largely melt, at least during the early stage of phenocryst deformation. A second reason may be the small grain-size of the groundmass, which would tend to promote grain-boundary-related processes of deformation like grain-boundary sliding, grain-boundary diffusion and pressure solution.

Microtonalite III was also sheared during intrusion, crystallization and at high-temperature subsolidus conditions during D2, as supported by the following points of evidence.

(1) Plagioclase phenocrysts are aligned with their flat faces parallel to the regional S2. Locally, the phenocrysts are fractured and dismembered, with K-feldspar between the fragments, probably grown from a melt.

(2) The plagioclase phenocrysts are partly recrystallized to polygonal and equidimensional grains, *ca.* 500–700 μm across. Such grain sizes are characteristic of temperatures of ~700–800°C (Kruhl 2001).

(3) Large grains of quartz show a strong chessboard pattern of subgrains, which develops only in high quartz. They point to deformation temperatures of *ca.* 620–670°C as a minimum, on the basis of 200–400 MPa pressure (Kruhl 1996).

(4) The grain boundaries of quartz are coarsely sutured, with segments of rhombohedral orientation. Such coarse suturing and crystallographic orientation are characteristic of amphibolite-facies and higher-temperature conditions (Voll 1969, Kruhl & Peternell 2002).

Indications of subsequent deformation during decreasing temperatures are given by the occurrence of recrystallized quartz with only prismatic subgrain-

boundaries around host grains with a chessboard pattern of subgrains. We infer that this deformation occurred in low quartz, *i.e.*, below *ca.* 620–670°C, given 200–400 MPa pressure (Kruhl 1996).

In the leucogranite (intrusive pulse IV), a well-developed solid-state deformation occurs, in the form of alignment of biotite, white mica and the flat faces of coarsely recrystallized lenses of quartz. Locally, recrystallized biotite, microcline twinning in K-feldspar, and partial replacement of microcline by myrmekite occur, all of which are consistent with solid-state deformation (*e.g.*, Vernon 2000, 2004). The parallelism of the solid-state deformation with a locally strong dimensional preferred orientation of plagioclase and microcline phenocrysts is consistent with magmatic flow before or continuous with solid-state deformation. The intrusion of magma thus coincided with regional deformation.

All the intrusive bodies have numerous indications of weak deformation during greenschist-facies conditions, which we interpret as the effect of the regional deformation during and after subsolidus cooling of the igneous rocks. Igneous plagioclase phenocrysts are bent and have albite and pericline deformation twins. Locally, coarsely recrystallized quartz is composed of prismatic subgrains and shows incipient fine recrystallization along the margins. Biotite is converted to chlorite along S3 planes. Quartz *c*-axis concentrations near the foliation pole, with angles of ~35° across strain *Z*, also indicate deformation during conditions of lowermost greenschist-facies regional metamorphism (Bouchez 1977, Kruhl 1998).

Conclusions

The Monte'e Senes complex in northeastern Sardinia represents a good example of a syntectonic sheeted igneous complex intrusive into a late-Variscan thrust regime during the collision of Gondwana and Armorica. The strict parallelism of D2 foliations and lineations of the wallrocks with the strong partly magmatic foliation and lineation of the mostly sheet-like intrusive bodies, together with the interference of D3 folding, and the inferred transition from magmatic to high-temperature, solid-state, kinematically corresponding deformation-induced structures, argue for a syntectonic intrusion and for a long-lasting history of intrusion during the regional D2 and D3 deformation events. It has been shown in the area north of Monte'e Senes that D2 and D3 occurred during a regime of decreasing temperatures; they probably are related to uplift of the northernmost External Nappe Zone of Sardinia. Therefore, the early tonalitic melts were injected after the temperature maximum into an already cooling crust, probably at medium-greenschist-facies conditions or even lower.

Acknowledgements

We dedicate this contribution to Dugald Carmichael, who has led us in new directions in metamorphic geology. We are grateful to Giacomo Oggiano for introducing us to the syntectonic tonalite sheets of northeastern Sardinia and for pointing to the Monte'e Senes complex as an interesting research object. We thank Phil Simony, Stephen Johnston, David R.M. Pattison and Robert F. Martin for critical comments. Field work and the first part of investigation took place during the stay of R. H. Vernon at the Technische Universität München as a Research Awardee of the Alexander von Humboldt Foundation. Investigation was continued during his second stay in München, again financially supported by the Humboldt Foundation. This support is gratefully acknowledged. In addition, the present study is related to a research project financially supported by the German Research Foundation (DFG) under grant KR 691/23–1. Thanks are also due to Klaus Haas for the preparation of the electronic versions of the figures, to Vladimir Ruttner for the preparation of thin sections, and to Mark Peternell for staining sample slabs.

References

Ashworth, J.A. (1972): Myrmekites of exsolution and replacement origins. *Geol. Mag.* **109**, 45-62.

Beccaluva, L., Civetta, L., Macciotta, G. & Ricci, C.A. (1985): Geochronology in Sardinia: results and problems. *In* Geochronology in Italy: Results and Problems (G. Fagnani, ed.). *Rend. Soc. It. Mineral. Petrol.* **40**, 57-72.

Bosworth, T.O. (1910): Metamorphism around the Ross of Mull Granite. *Quart. J. Geol. Soc. London* **66**, 376-396.

Bouchez, J.-L. (1977): Plastic deformation of quartzites at low temperature in an area of natural strain gradient. *Tectonophysics* **39**, 25-50.

Cappelli, B., Carmignani, L., Castorina, F., Di Pisa, A., Oggiano, G. & Petrini, R. (1991): A Hercynian suture zone in Sardinia: geological and geochemical evidence. *Geodinamica Acta* **5**, 101-118.

Carmignani, L., Carosi, R., Di Pisa, A., Gattiglio, M., Musumeci, G., Oggiano, G. & Pertusati, P.C. (1994): The Hercynian chain in Sardinia (Italy). *Geodinamica Acta* **7**, 31-47.

_____, _____, Disperati, L., Funeda, A., Musumeci, G., Pasci, S. & Pertusati, P.C. (1992): Tertiary transpressional tectonics in NE Sardinia, Italy. *In* Contributions to the Geology of Italy (L. Carmignani & F.P. Sassi, eds.). *IGCP 276, Newsletter* **5**, 83-96.

_____, Francescelli, M., Pertusati, P.C. & Ricci, C.A. (1980): Evoluzione tettonico-metamorfica del basamento ercinico della Nurra (Sardegna NW). *Mem. Soc. Geol. It.* **20**, 57-84.

DEL MORO, A., DI SIMPLICIO, P., GHEZZO, C., GUASPARRI, G., RITA, F. & SABATINI, G. (1975): Radiometric data and intrusive sequence in the Sardinian batholith. *Neues Jahrb. Mineral., Abh.* **126**, 28-44.

EUGSTER, H. P. (1970): Thermal and ionic equilibria among muscovite, K-feldspar and aluminosilicate assemblages. *Fortschr. Mineral.* **47**, 106-123.

FRANCESCELLI, M., MEMMI, I., PANNUTI, F. & RICCI, C.A. (1989): Diachronous metamorphic equilibria in the Hercynian basement of northern Sardinia, Italy. *In* Evolution of Metamorphic Belts (J.S. Daly, R.A. Cliff & B.W.D. Yardley, eds.). *Geol. Soc. London, Spec. Publ.* **43**, 371-375.

_____, _____ & RICCI, C.A. (1982): Zoneografia metamorfia della Sardegna settentrionale. *In* Guida alla Geologia del Paleozoico Sardo (L. Carmignani, T. Cocozza, C. Ghezzo, P.C. Pertusati & C.A. Ricci, eds.). *Mem. Soc. Geol. It.* **24**, *Suppl.* **B**, 137-149.

HELBING, H. & KRUHL, J.H. (2000): Compressional, extensional and strike-slip tectonics along a late-Variscan crustal-scale suture in north-east Sardinia. *Geophys. Abstr.* **2/2000**.

JI, SHAOCHENG & MAINPRICE, D. (1988): Natural deformation fabrics of plagioclase: implications for slip systems and seismic anisotropy. *Tectonophysics* **147**, 145-163.

KRUHL, J.H. (1987): Zur Deformation und Gitterregelung des Plagioklases. *Jahrb. Geol. B.-A., Wien*, **130/2**, 205-243.

_____ (1996): Prism- and basal-plane parallel subgrain boundaries in quartz: a micro-structural geothermobarometer. *J. Metamorph. Geol.* **14**, 581-589.

_____ (1998): Prism- and basal-plane parallel subgrain boundaries in quartz: a microstructural geothermobarometer – discussion and reply. *J. Metamorph. Geol.* **16**, 142-146.

_____ (2001): Crystallographic control on the development of foam textures in quartz, plagioclase and analogue material. *Int. J. Earth Sci.* **90**, 104-117.

_____ & HUNTEMANN, T. (1991): The structural state of the former lower continental crust in Calabria (S. Italy). *Geol. Rundsch.* **80**, 289-302.

_____ & PETERNELL, M. (2002): The equilibration of high-angle grain boundaries in dynamically recrystallized quartz: the effect of crystallography and temperature. *J. Struct. Geol.* **24**, 1125-1137.

LISTER, G.S. & DORNSIEPEN, U.F. (1982): Fabric transitions in the Saxony granulite terrain. *J. Struct. Geol.* **4**, 81-92.

MEMMI, I., BARCA, S., CARMIGNANI, L., COCCOZZA, T., ELTER, F.M., FRANCESCELLI, M., GATTIGLIO, M., GHEZZO, C., MINZONI, N., NAUD, G., PERTUSATI, P. & RICCI, C.A. (1983): Further geochemical data on the Pre-Hercynian igneous activities of Sardinia and on their geodynamic significance. *IGCP 5, Newsletter* **5**, 87-93.

MILLER, R.B. & PATERSON, S.R. (1994): The transition from magmatic to high temperature solid-state deformation: implications from the Mount Stuart batholith, Washington. *J. Struct. Geol.* **16**, 853-865.

NABHOLZ, W.K. & VOLL, G. (1963): Bau und Bewegung im gotthardmassivischen Mesozoikum bei Ilanz (Graubünden). *Eclog. Geol. Helv.* **56**, 755-808.

PATTISON, D.R.M. (1992): Stability of andalusite and sillimanite and the Al_2SiO_5 triple point: constraints from the Ballachulish aureole, Scotland. *J. Geol.* **100**, 423-446.

_____, SPEAR, F.S., DEBUHR, C.L., CHENEY, J.T. & GUIDOTTI, C.V. (2002): Thermodynamic modelling of the reaction muscovite + cordierite → Al_2SiO_5 + biotite + quartz + H_2O: constraints from natural assemblages and implications for the metapelitic petrogenetic grid. *J. Metamorph. Geol.* **20**, 99-118.

_____ & TRACY, R.J. (1991): Phase equilibria and thermobarometry of metapelites. *In* Contact Metamorphism (D.M. Kerrick, ed.). *Rev. Mineral.* **26**, 105-206.

PHILLIPS, E.R. (1974): Myrmekite — one hundred years later. *Lithos* **7**, 181-194.

_____ (1980): On polygenetic myrmekite. *Geol. Mag.* **17**, 29-36.

_____, RANSOM, D.M. & VERNON, R.H. (1972): Myrmekite and muscovite developed by retrograde metamorphism at Broken Hill, New South Wales. *Mineral. Mag.* **38**, 570-578.

ROSENBERG, C.L. & STÜNITZ, H. (2003): Deformation and recrystallization of plagioclase along a temperature gradient. An example from the Bergell tonalite. *J. Struct. Geol.* **25**, 389-408.

SANDER, B. (1930): *Gefügekunde der Gesteine*. Springer-Verlag, Wien, Austria.

SHELLEY, D. (1993): *Igneous and Metamorphic Rocks under the Microscope.* Chapman & Hall, London, U.K.

VERNON, R.H. (1975): Microstructural interpretation of some fibrolitic sillimanite aggregates. *Mineral. Mag.* **40**, 303-306.

_____ (1979): Formation of late sillimanite by hydrogen metasomatism (base-leaching) in some high-grade gneisses. *Lithos* **12**, 143-152.

_____ (1986): K-feldspar megacrysts in granites – phenocrysts, not porphyroblasts. *Earth-Sci. Rev.* **23**, 1-63.

_____ (1987a): Oriented growth of sillimanite in andalusite, Placitas – Juan Tabo area, New Mexico, U.S.A. *Can. J. Earth Sci.* **24**, 580-590.

_____ (1987b): Growth and concentration of fibrous sillimanite related to heterogeneous deformation in K-feldspar – sillimanite metapelites. *J. Metamorph. Geol.* **5**, 51-68.

_____ (1991): Questions about myrmekite in deformed rocks. *J. Struct. Geol.* **13**, 979-985.

_____ (2000): Review of microstructural evidence of magmatic and solid-state flow. *Electronic Geosci.* **5**(2).

_____ (2004): *A Practical Guide to Rock Microstructure.* Cambridge University Press, Cambridge, U.K.

VOLL, G. (1960): New work on petrofabrics. *Liverpool Manch. Geol. J.* **2/3**, 503-567.

_____ (1969): *Klastische Mineralien aus den Sedimentserien der Schottischen Highlands und ihr Schicksal bei aufsteigender Regional- und Kontaktmetamorphose.* Habilitationsschrift, Fakultät für Bergbau und Hüttenwesen, Technische Universität Berlin, D83.

VOLLAND, S. (1999): *Geologie und fraktale Geometrie an spät- bis postvariszischen Bruchstrukturen in der S-Nurra/NW-Sardinien*. Diploma thesis, Technische Universität München.

WINTSCH, R.P. (1975): Solid-fluid equilibria in the system $KAlSi_3O_8$–$NaAlSi_3O_8$–Al_2SiO_5–SiO_2–H_2O–HCl. *J. Petrol.* **16**, 57-79.

Received November 28, 2003, revised manuscript accepted November 25, 2004.